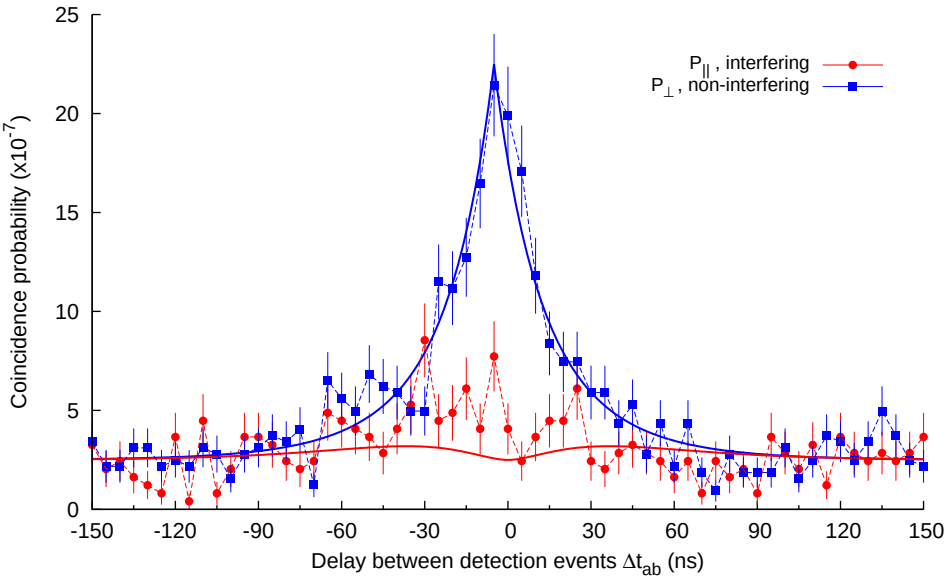

Figure 1: Coincidence probability between the two arms of the interferometer conditioned on the detection of a trigger photon. The squares (blue) shows the non-interfering case: the photons from the FWM are horizontally polarized and the photons from the single atom are vertically polarized. The circles (red) shows the interfering case: both the photons are horizontally polarised. The time delay between the peak amplitude is adjusted to be $\Delta t \approx 0$ ns. The probability is obtained from a time distribution histogram of triple coincidences between the detectors D_t, D_a and D_b normalized to the total number of triggers registered by D_t. The interference visibility for an integration window of $-12.5\,\text{ns} \leq \Delta t_{ab} \leq 12.5\,\text{ns}$ is 74±4%, and it reduces to 66±4% when the window width is increased to $-25\,\text{ns} \leq \Delta t_{ab} \leq 25\,\text{ns}$. The solid lines represents the expected shape from the theoritical model: $P_{\perp}(\Delta t_{ab}) = bg + \eta\, r_1$ for the blue line and $P_{||}(\Delta t_{ab}) = bg + \eta\, r_2$ for the red line. The efficiency $\eta = 0.00016$ agrees with the single photon efficiencies, $\eta \approx \eta_{sa}\,\eta_{fwm}$ and $bg = 2.5 \times 10^{-7}$ is due to accidental coincidences.

We measure the coincidences between the detector events on D_a and D_b if a click was registered on D_t within a time window of $\Delta t_f \leq \Delta t_{ta} \leq (\Delta t_f + 85\,\text{ns})$, where t_f is the fiber delay. This time window was chosen such that more than 95% of the photons from the single-atom and 99.5% of the photons from FWM is detected within this window. The coincidences are resolved into time-bins of width 5 ns. The total number of coincidences $N_{ab|t}$ are normalized to the total trigger events N_t in the measurement time. This gives the conditioned probability of detecting a coincidence,

$$P(\Delta t_{ab}) = \frac{N_{ab|t}(\Delta t_{ab})}{N_t} \tag{1}$$

The two photons are maximally indistinguhable when they have idential polarizations and the time delay between their peak ampilitudes, $\Delta t = 0$ ns. We obtain the coincidence probability $P_{||}$ under this condition by choosing horizontal polarization for both the incident photons. For comparison with the case when the two photons are completely distinguishable, we measure the coincidence probability $P_{\perp}$ when the two photons have orthogonal polarisations. Figure 1 shows $P_{||}$ and $P_{\perp}$ as a function of the detection time delay between D_a and D_b. The normalized probability, P^n is defined as

$$P^n = \int_{T_c} \frac{P_{||}}{P_{\perp}}\, d(\Delta t_{ab}) \tag{2}$$

where T_c is the integration time window. The interference visibility, $V = 1 - P^n$.

The coincidence probability can be theoritically estimated from the wavefunctions of the two interfering photons, $\psi_{fwm}(t)$ and $\psi_{sa}(t - \Delta t)$ (see suplementary information / methods). In the non-interfering

case the probability of a coincidence as a function of the detection time difference Δt_{ab} is given by,

$$r_1(\Delta t_{ab}) \;=\; \frac{1}{4}\int_{-\infty}^{\infty} [\psi_{fwm}(t)\,\psi_{sa}(t-\Delta t+\Delta t_{ab})]^2 \;+\; [\psi_{fwm}(t+\Delta t_{ab})\,\psi_{sa}(t-\Delta t)]^2\,dt \tag{3}$$

and in the interfering case the coincidence probability is given by,

$$r_2(\Delta t_{ab}) \;=\; r_1(\Delta t_{ab}) \;-\; \frac{1}{2}\int_{-\infty}^{\infty} \psi_{fwm}(t)\,\psi_{sa}(t-\Delta t+\Delta t_{ab})\,\psi_{fwm}(t+\Delta t_{ab})\,\psi_{sa}(t-\Delta t)dt \tag{4}$$

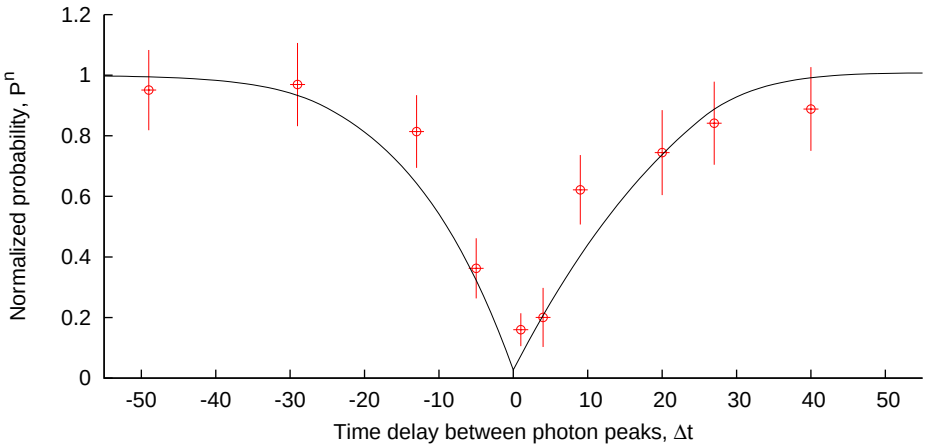

Figure 2: Normalized probability P^n as a function of the delay between the peaks amplitudes of the two photons. For each point P^n is obtained after correcting for the accidental background (see methods section). The solid line is from the theoritical model assuming a perfect spatial mode overlap of the photons (see Eq. (5))

Traditionally a HOM dip in the normalized probability P^n is obtained by gradually delaying the arrival one photon with respect to the other at the BS. In all the previously reported measurements of the HOM dip the coherence times of the photons were much shorter than the coincidence window, and the dip could be observed by using the same window for all the delays. However in our case the coincidence window time is shorter than the coherence time of the photons. Therefore the chosen window depends on the delay Δt. The plot of P^n by varying the delay Δt is shown in figure.... For every point the integration window for $P_{||}(\Delta t_{ab})$ is chosen to be ± 25 ns around the delay time $\pm\Delta t$. For all the delays the normalization term in the denominator of Eq.(2) is obtained from the $P_\perp$ shown in figure figure 1 with an integration window of ± 25 ns around $\Delta t_{ab} = 0$ ns. This is explained in more detail in the supplementary information / methods section.

The theoritically expected shape of the HOM dip is obtained from Eq. (3) and (4),

$$P^n(\Delta t) \;=\; \frac{\int_{T_c} r_2\, d(\Delta t_{ab})}{\int_{-25\,ns}^{25\,ns} r_1\, d(\Delta t_{ab})} \tag{5}$$

where integration window T_c is the same window used for the experimental points.

Methods / Supplementary:

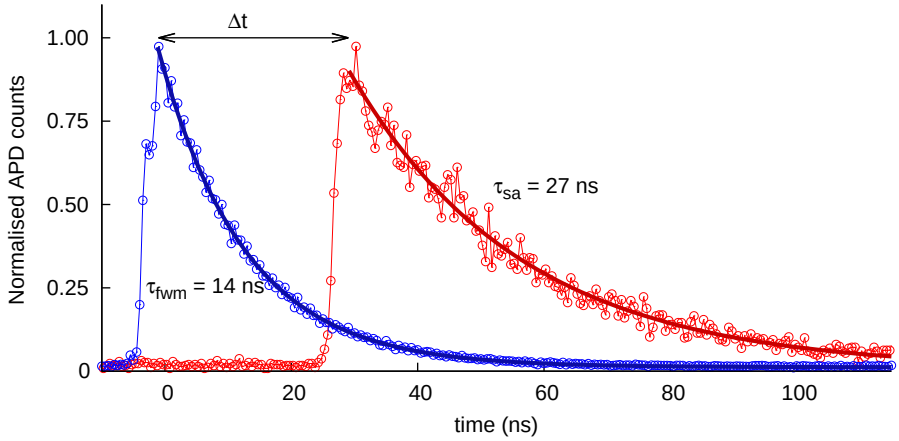

Figure 3: The normalized coincidences between D_t and D_a when $\Delta t = -30\,\text{ns}$. The x-axis is corrected for the cable and the fiber delays.

The wavefunctions of the photons from the FWM and the SA are given by,

$$\psi_{fwm}(t) = \frac{1}{\sqrt{\tau_{fwm}}} e^{-\frac{t}{2\,\tau_{fwm}}}\,\Theta(t) \tag{6}$$

$$\psi_{sa}(t - \Delta t) = \frac{1}{\sqrt{\tau_{sa}}} e^{-\frac{(t-\Delta t)}{2\,\tau_{sa}}}\,\Theta(t - \Delta t) \tag{7}$$

where t is the arrival time of the photons at the beam splitter, τ_{sa} and τ_{fwm} are coherence times of the photons, and Δt is the delay between the peak amplitudes of the photons.

A coincidence event between the detectors D_a and D_b happens if both the photons are either transmitted or reflected at the beam splitter as shown in figure 4.

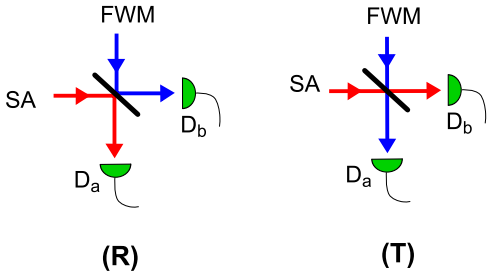

Figure 4: The two situations that can result in a coincidence between the detectors D_a and D_b: (R) Both the photons are reflected at the BS. (T) Both the photons are transmitted through the BS.

When the delay $|\Delta t| > 0$, the two scenarios for coincidence between D_a and D_b shown in figure 4 manifests as twin peaks in $P_{||}(\Delta t_{ab})$ separated by a time delay of $2\,\Delta t$. This is shown in figure 5 for $\Delta t = -14\,\text{ns}$ and $\Delta t = -30\,\text{ns}$. In this situation the integration window to compute the visibility has to be moved to be centered around the peaks. As it can be seen the total width of the integration window is now increased compared to the case when $\Delta t = 0\,\text{ns}$, and this results in increased values accidental background for these points.

The plot of normalized probability P^n as a function of the delay time without correcting for the accidentals is shown in the figure 6. Due to the unequal values of the total accidental background for each point, P^n tends to 1.3 for $\Delta t >> 0$ instead of 1. We therfore have to subtract the accidental background to be able to compare the experimental points to the expected theory (see figure 2).

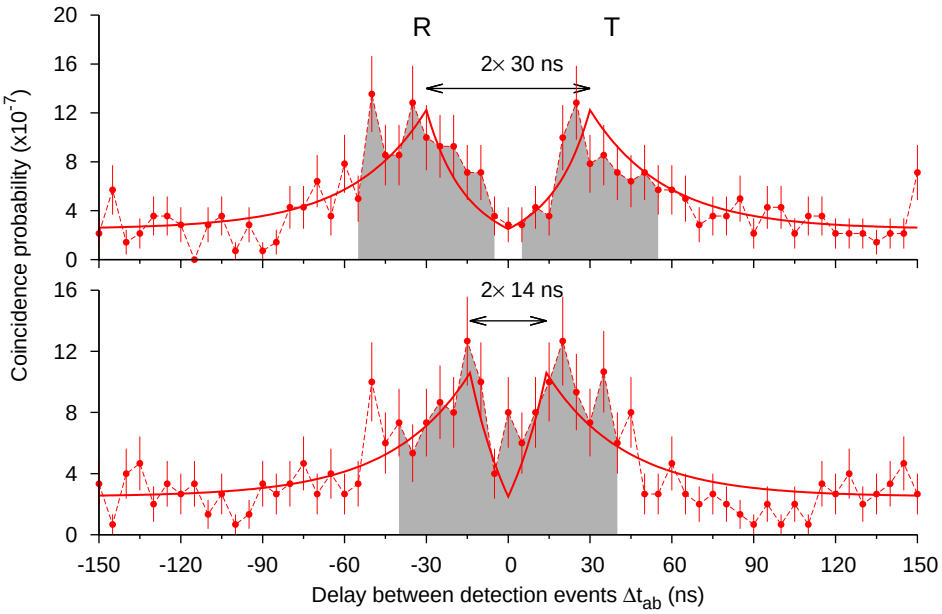

Figure 5: The coincidence probability for $|\Delta t| > 0$. The two peaks at $\Delta t_{ab} = \pm\Delta t$ is from the two possible situations to observe coincidence shown in figure 4. The integration window for $P_{||}$ is shown as grey shaded region. When $\Delta t \geq 25\,\text{ns}$ the window is split into two regions $\pm 25\,\text{ns}$ wide around the peaks as seen in the top plot. When $\Delta t < 25\,\text{ns}$ we have a continuous window of $(-|\Delta t| - 25\,\text{ns}) \leq \Delta t_{ab} \leq (|\Delta t| + 25\,\text{ns})$. The solid lines are obtained from the theoritical model described in the main text, with the integration windows chosen in the same way as the experimental points.

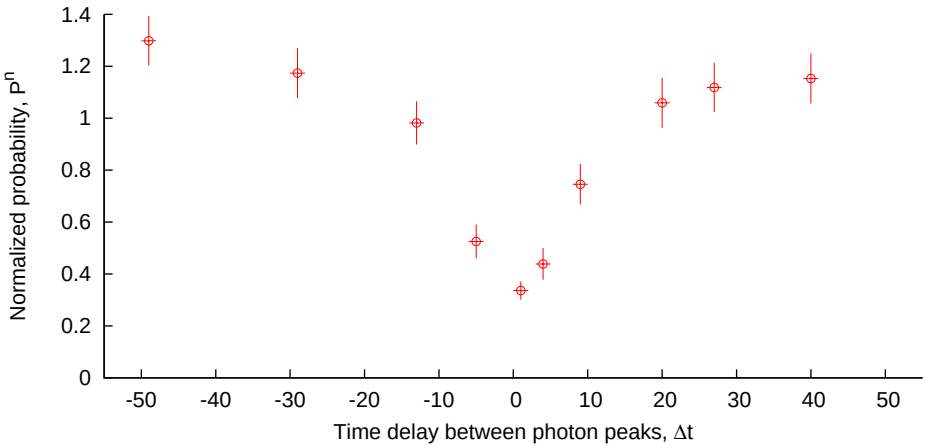

Figure 6: The HOM dip in the visibility without subtracting the accidental background.